COHESIVE ZONE MODEL FOR DEBOND FAILURE IN PLATED BEAM USING TRANSVERSE SHEAR DEFORMATION THEORY

Lalitha Chattopadhyay and T. Sivaranjani

Structural Technologies Division, CSIR- National Aerospace Laboratories, Bangalore, India
Email: lalitha@css.nal.res.in

Received 14 February 2011; accepted 19 August 2011

ABSTRACT

The interfacial shear stress is obtained in a plated beam using cohesive zone integrated analytical method. The shear stress distribution is obtained in elastic and elastic-softening zone. The plate- end debond initiation along with debond load is calculated using higher order theory including the transverse shear deformations of both the beam and the plate. The closed-form expression for interface shear stress is used to estimate the influence of different material parameters on the length of the softening zone and debond initiation. A complete solution for debond initiation is presented for the case of a simply supported beam along with the general formulation of the governing differential equations for the interfacial shear stresses and the results are verified with literature values.

Keywords: Cohesive zone model, transverse shear, plated beam, debond

1 INTRODUCTION

Debonding failures starting from a plate-end depend largely on the concentration of interfacial shear and normal stresses between the beam and the bonded plate in the vicinity of the plate-end. The determination of these interfacial stresses in the elastic range has been extensively researched in the literature. Smith and Teng (2001) presented a review of the approximate closed-form solutions for interfacial stresses with a new solution for application to beams bonded to thin plate. Rabinovich and Frostig (2000) gave closed-form high-order analyses of reinforced beams strengthened with FRP plates, which satisfy the free surface condition at the ends of the adhesive layer. The closed-form solution is presented by Laura De Lorenzis et.al (2009) provides the interfacial behavior along the plate during subsequent stages of loading. Ninoslav Pesic (2003) studied the problem of early concrete cover delamination and plate-end failure of reinforced concrete beams strengthened with externally bonded FRP-reinforcement. Fabrizio Greco (2007) provides an enhanced analytical model for the analysis of typical edge debonding problems with externally bonded composite laminated plates induced by interface fracture phenomena. Debonding growth is studied in the framework of Fracture Mechanics. The use of nodal analysis and Galerkin's method are given by Bouchikhi et.al (2010) for the calculation of interfacial shear stresses of beams strengthened with CFRP plates with tapered end. Elastic interfacial stress including the adherend shear deformation for simply supported plated beam is given by Tounsi Abdelouahed (2006). The objective of the present work is to incorporate the plate and beam shear deformations into the interfacial shear stress distribution

and to determine these stresses in elastic stage, elastic-softening and debond initiation stage along with plate-end debond initiation load.

2 PLATE-END DEBONDING

Plate-end debonding initiates at the end of the bonded plate and propagates towards midspan of the plate. This debonding can be characterized as interfacial debonding and this type of plate-end debonding is mainly caused by high stresses at the end of the plate. We consider a simply supported beam with rectangular cross-section of width b_1 and depth h_1 and subjected to a point load P at mid-span as shown in the Figure 1. A thin plate of width b_2, thickness h_2, and length l is bonded to the beam by adhesive layer. Let E_1 and E_2 are respectively the elastic moduli of the beam and the plate. The following assumptions are adopted in the analysis presented in this study: (a) the materials involved in the problem are linearly elastic and the non-linearity is concentrated at the interface; (b) the stresses in the adhesive layer are uniform across its thickness.

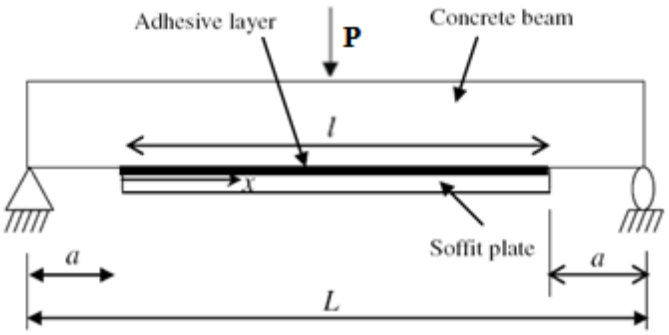

Figure 1: Simply supported plated beam under a midspan force

3 COHESIVE ZONE MODEL

The shear cohesive law implemented herein is bilinear. This law is assumed to be antisymmetric for relative displacements of opposite signs, and only the portion of the curve for positive δ is reported in Figure 2. The bilinear shape is able to capture the three characteristic parameters of the interface, i.e. the fracture energy (area underneath the curve), the cohesive strength, and the linear elastic properties (slope of the curve in the ascending branch). The following analytical relationships represent the cohesive law of Figure 2

$$\tau = \begin{cases} K\delta & \text{for } 0 \le \delta \le \frac{\tau_p}{K} \\ \frac{K}{k_\delta - 1}\left(\frac{k_\delta \tau_p}{K} - \delta\right) & \text{for } \frac{\tau_p}{K} \le \delta \le k_\delta \frac{\tau_p}{K} \\ 0 & \text{for } \delta \ge k_\delta \frac{\tau_p}{K} \end{cases} \quad (1)$$

where the three branches of the law can respectively be labeled as elastic, softening, and debonding. In the above equations, δ_p and δ_u are, respectively, the value at peak shear stress and the ultimate value (at zero shear stress) of the tangential relative displacement and τ_p is the peak value of the shear stress.

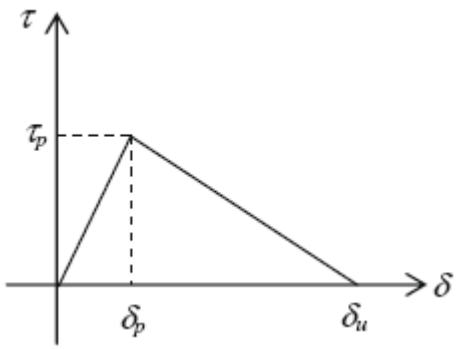

Figure 2: Interfacial (shear) cohesive law

4 ANALYTICAL APPROACH FOR INTERFACE STRESS INCLUDING TRANSVERSE SHEAR DEFORMATION

The plate-beam interface is assumed to be a layer of adhesive having a constitutive behavior under shear and tension given by cohesive laws of the desired shape. In this paper, for analytical CZ modeling of interfacial stresses in plated beams, we have considered only shear stresses. For the sake of simplicity, the interfacial shear stresses (τ) is termed as "interfacial stresses"; the tangential relative displacements across the interface (δ), is termed as "relative displacements"; cohesive law relating τ and δ, is indicated simply as "cohesive law"; and so forth.

4.1 Governing Equations

A differential section (dx) is cut out from the plate strengthened beam as shown in Figure 3. The composite beam is made of three materials: beam material, adhesive layer material and plate material. In the present analysis linear elastic behavior is assumed for all the materials. The adhesive is considered only in transferring the stresses from the beam to the plate. In the differential segment of a plated beam shown in Figure 3, the interfacial shear and normal stresses are denoted by $\tau(x)$ and $\sigma(x)$, respectively. Figure 3 also shows the positive sign convention for the bending moment, shear force, axial force and applied loading. As a result of the above assumption, the beam and the plate are subjected to an axial force, N (taken as positive in compression), a shear force, V, and a bending moment, M which are the functions of the coordinate x along the beam axis. The interfacial shear stress, $\tau(x)$, acts at the interfaces between beam and adhesive and between adhesive and plate, as well as on the adhesive element which is subjected to pure shear. The shear stress is assumed to be uniform across the adhesive thickness.

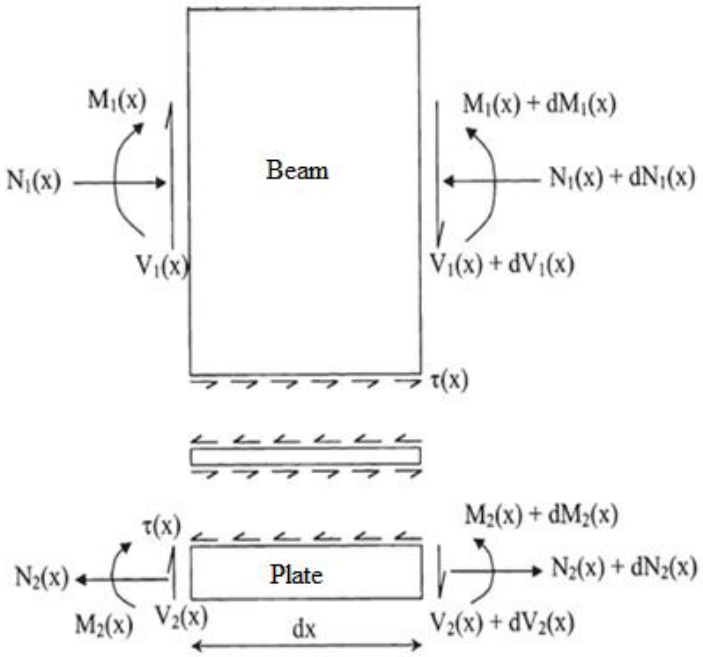

Figure 3: Differential element of the plated beam

From Figure 3, the following equilibrium equations for interfacial stress are obtained

$$\frac{dM_1(x)}{dx} = \frac{R}{R+1}[V_T(x) - b_2\tau(x)(y_1 + y_2 + t_a)] \tag{2}$$

$$\frac{dM_2(x)}{dx} = \frac{1}{R+1}[V_T(x) - b_2\tau(x)(y_1 + y_2 + t_a)] \tag{3}$$

Where $R = \frac{E_1 I_1}{E_2 I_2}$

$$\frac{dN_1(x)}{dx} = -b_2\tau(x) \tag{4}$$

$$\frac{dN_2(x)}{dx} = b_2\tau(x) \tag{5}$$

The tangential displacements of beam and plate including the transverse shear deformation of the beam and the plate are given by the following equations

$$\frac{d^2u_1}{dx^2} = \frac{y_1}{E_1 I_1}\frac{dM_1(x)}{dx} + \frac{1}{E_1 A_1}\frac{dN_1(x)}{dx} + \frac{t_1}{3G_1}\frac{d^2\tau}{dx^2} \tag{6}$$

$$\frac{d^2u_2}{dx^2} = -\frac{y_2}{E_2 I_2}\frac{dM_2(x)}{dx} + \frac{1}{E_2 A_2}\frac{dN_2(x)}{dx} - \frac{t_2}{3G_2}\frac{d^2\tau}{dx^2} \tag{7}$$

4.2 Elastic (*E*) Stage

In this section, using the first branch of the cohesive law for elastic range and the above governing equations we get interfacial stress distribution

$$\tau_e(x) = K[u_2 - u_1] \tag{8}$$

From the above tangential cohesive law for elastic stage and from the bending equation of the beam we get the following differential equation for the shear stress distribution in the elastic zone,

$$\frac{d^2\tau_e(x)}{dx^2} + \lambda_e^2\tau_e(x) - J_e V_T(x) = 0 \tag{9}$$

where,

$$\lambda_e^2 = \left[\frac{(y_1+y_2)(y_1+y_2+t_a)}{E_1I_1+E_2I_2} + \frac{1}{E_1A_1} + \frac{1}{E_2A_2}\right]\frac{b_2}{I_e} \tag{10}$$

$$I_e = \frac{1}{K} + \frac{t_1}{3G_1} + \frac{t_2}{3G_2}, J_e = \left[\frac{y_1+y_2}{E_1I_1+E_2I_2}\right]\frac{1}{I_e}, V_T(x) = \frac{P}{2} \tag{11}$$

The general solution of the differential equation (9) is given by,

$$\tau_e(x) = C_1\cosh(\lambda_e x) + C_2\sinh(\lambda_e x) + \frac{J_e P}{2\lambda_e^2} \qquad 0 \le x \le l/2 \tag{12}$$

The boundary conditions are (a) the shear stress is zero on the symmetry axis, $x = l/2$ (b) at the plate-end $x = 0$, the axial force is zero $N_1 = N_2 = 0$, for both beam and plate. Using the first boundary condition we have,

$$At\ x = {}^{l}/_{2}; \qquad \tau_e(x) = 0 \tag{13}$$

Using the second boundary condition we get,

$$At\ x = 0; \qquad N_1 = 0, N_2 = 0, M_1 = \frac{Pa}{2}, M_2 = 0 \tag{14}$$

From the boundary conditions in equation (13) & (14), the unknown constants of integration are calculated and given by,

$$C_1 = \frac{1}{\cosh\left(\lambda_e\frac{l}{2}\right)}\left[\frac{1}{\lambda_e I_e}\frac{y_1}{E_1I_1}\frac{Pa}{2}\sinh\left(\lambda_e\frac{l}{2}\right) - \frac{J_e P}{2\lambda_e^2}\right];\ C_2 = -\frac{1}{\lambda_e I_e}\frac{y_1}{E_1I_1}\frac{Pa}{2} \tag{15}$$

4.3 Elastic – Softening (*ES*) Stage

As the load increases, the interfacial shear stress increases and reaches the maximum value τ_p at $x = 0$. Once τ reaches the maximum value, softening starts at the termination of the plate

and the remaining region of the plate are in elastic phase. At the beginning of this phase, the softening zone length $\bar{x}$ increases for further increase in the applied load. In the softening zone, ($0 \le x \le \bar{x}$), using the second branch of the cohesive law we get interfacial stress distribution in the elastic-softening zone as given by the following procedure. The cohesive law for elastic-softening zone is given by,

$$\tau_s(x) = \frac{K}{k_\delta - 1}\left[\frac{k_\delta \tau}{K} - u_2 - u_1\right] \qquad (0 \le x \le \bar{x}) \tag{16}$$

From the above tangential cohesive law we get the following differential equation for the shear stress distribution in the elastic-softening zone as given by,

$$\frac{d^2\tau_s(x)}{dx^2} + \lambda_s^2\tau_s(x) - J_s V_T(x) = 0 \tag{17}$$

Where

$$\lambda_s^2 = \left[\frac{(y_1+y_2)(y_1+y_2+t_a)}{E_1I_1+E_2I_2} + \frac{1}{E_1A_1} + \frac{1}{E_2A_2}\right]\frac{b_2}{I_s},\ I_s = \frac{k_\delta - 1}{K} - \frac{t_1}{3G_1} - \frac{t_2}{3G_2}$$

$$J_s = \left[\frac{y_1+y_2}{E_1I_1+E_2I_2}\right]\frac{1}{I_s},\ V_T(x) = \frac{P}{2}$$

General solutions for the interfacial shear stresses

$$\tau_s(x) = C_3\cos(\lambda_s x) + C_4\sin(\lambda_s x) + \frac{J_s V_T(x)}{\lambda_s^2} \qquad 0 \le x \le \bar{x} \tag{18}$$

$$\tau_a(x) = C_5\cosh(\lambda_a x) + C_6\sinh(\lambda_a x) + \frac{J_a V_T(x)}{\lambda_a^2} \qquad \bar{x} \le x \le l/2 \tag{19}$$

The boundary conditions are (a) the shear stress is zero on the symmetry axis, $x = l/2$ (b) at the plate-end $x = 0$, the axial force is zero $N_1 = N_2 = 0$, for both beam and plate. Using the first boundary condition we have,

$$At\ x = {}^{l}/_{2}; \qquad \tau_a(x) = 0 \tag{20}$$

Using the second boundary condition we get,

$$At\ x = 0; \qquad N_1 = 0, N_2 = 0, M_1 = \frac{Pa}{2}, M_2 = 0 \tag{21}$$

From the stress continuity condition at $x = \bar{x}$, we get the following equations for shear stress distribution.

$$At\ x = \bar{x}; \qquad \tau_a(x) = \tau_s(x), \quad \tau_a(x) = \tau_p \tag{22}$$

Applying the boundary and continuity conditions in equation (21) – (22), the constants of integrations are determined as follows:

$$C_3 = \frac{1}{\cos(\lambda_s \bar{x})}\left[\tau_p - \frac{J_s V_T(x)}{\lambda_s^2} - \frac{1}{\lambda_s I_s}\frac{y_1}{E_1 I_1}\frac{Pa}{2}\sin(\lambda_s \bar{x})\right]$$

$$C_4 = \frac{1}{\lambda_s I_s}\frac{y_1}{E_1 I_1}\frac{Pa}{2}$$

$$C_5 = \frac{1}{\sinh[\lambda_e(\bar{x}-l/2)]}\left[\frac{J_e V_T(x)}{\lambda_e^2}\left[\sinh\left(\lambda_e \frac{l}{2}\right) - \sinh(\lambda_e \bar{x})\right] - \tau_p \sinh\left(\lambda_e \frac{l}{2}\right)\right] \quad (23)$$

$$C_6 = \frac{1}{\sinh[\lambda_e(l/2-\bar{x})]}\left[\frac{J_e V_T(x)}{\lambda_e^2}\left[\cosh\left(\lambda_e \frac{l}{2}\right) - \cosh(\lambda_e \bar{x})\right] - \tau_p \cosh\left(\lambda_e \frac{l}{2}\right)\right]$$

The point of transition between elastic and softening regions is determined by equating the derivatives of elastic and softening shear stress components and these stress components are given by the following expressions

$$\frac{d\tau_e(\bar{x})}{dx} = K\left[-\frac{y_2}{E_2 I_2}M_2(\bar{x}) + \frac{N_2(\bar{x})}{E_2 A_2} - \frac{t_2}{3G_2}\frac{d\tau(x)}{dx} - \frac{y_1}{E_1 I_1}M_1(\bar{x}) + \frac{N_1(\bar{x})}{E_1 A_1} - \frac{t_1}{3G_1}\frac{d\tau(x)}{dx}\right] \quad (24)$$

$$\frac{d\tau_s(\bar{x})}{dx} = -\frac{1}{k_\delta - 1}K\left[-\frac{y_2}{E_2 I_2}M_2(\bar{x}) + \frac{N_2(\bar{x})}{E_2 A_2} - \frac{t_2}{3G_2}\frac{d\tau(x)}{dx} - \frac{y_1}{E_1 I_1}M_1(\bar{x}) + \frac{N_1(\bar{x})}{E_1 A_1} - \frac{t_1}{3G_1}\frac{d\tau(x)}{dx}\right] \quad (25)$$

Equating the derivatives we get the following equation for determining $\bar{x}$,

$$\frac{d\tau_s(\bar{x})}{dx} = -\frac{1}{k_\delta - 1}\frac{d\tau_e(\bar{x})}{dx} \quad (26)$$

From the above equation (26) we get the implicit expression for $\bar{x}$ in terms of applied load, material and geometric properties as given by,

$$-\frac{\lambda_e \tau_p}{k_\delta - 1}\coth\left[\lambda_e\left(\bar{x} - l/2\right)\right] - \frac{J_e P}{2\lambda_e(k_\delta - 1)\sinh\left[\lambda_e(\bar{x} - l/2)\right]} + \tan(\lambda_s \bar{x})\left[\tau_p \lambda_s - \frac{J_s P}{2\lambda_s} - \frac{Pa y_1 \sin(\lambda_s \bar{x})}{2E_1 I_1 I_s}\right] - \frac{Pa y_1 \cos(\lambda_s \bar{x})}{2E_1 I_1 I_s} = \frac{J_e P}{2\lambda_e(k_\delta - 1)} \quad (27)$$

4.4 Debond Failure

The debond initiates at the point where the shear stress vanishes and the corresponding shear stress distribution at this point is given by the following expression by substituting the value $x = \bar{x}_D$. At the debond initiation point we have the following condition,

at $x = 0$, $\tau_s(x) = 0$ (28)

$$\tau_s(0) = C_3 + \frac{J_s P}{2\lambda_s^2} \tag{29}$$

Then by using eqn. (23) on eqn. (29), the plate-end debond initiation point $\bar{x}_D$ is given by the following implicit relation,

$$P = 2\lambda_s \tau_p \frac{1}{\left[\frac{J_s}{\lambda_s}\left(1-\cos(\lambda_s \bar{x}_D)+\frac{y_1 a}{I_s I_1 E_1}\sin(\lambda_s \bar{x}_D)\right)\right]} \tag{30}$$

From the above equation (30), we get the corresponding plate-end debond load.

Figure 4 gives the interfacial shear stress distribution in elastic-softening-debond initiation stage.

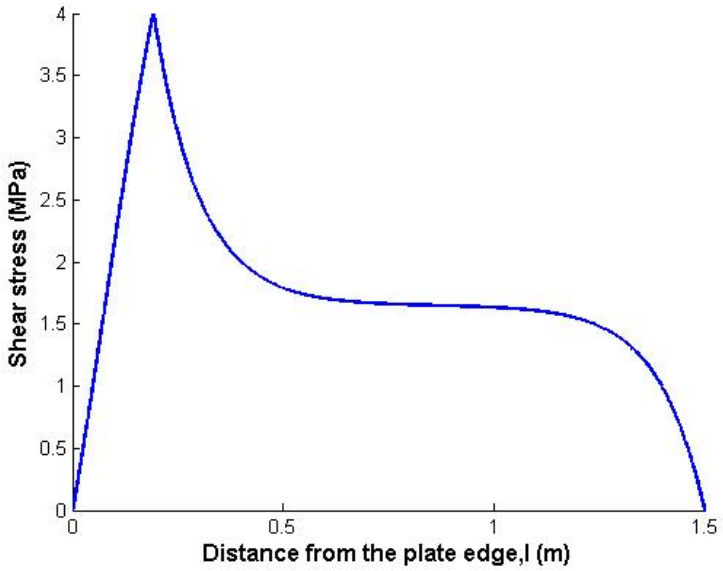

Figure 4: Elastic Softening and Debonding stage at 2.5 kN

5 RESULTS AND DISCUSSIONS

The effect of the beam and the plate transverse shear stiffness on the maximum shear stress is examined by comparing the results obtained with the present theory and those determined in (Lorenzis 2009). In the present work, beam strengthened with a glass–fiber reinforced plastic (GFRP), CFRP or steel soffit plate is analyzed. The beams are simply supported and subjected to a central point load. A summary of the geometric and material properties is given in Table 1. The span of beam is L = 3600 mm, the distance from the support to the end of the plate is a = 300 mm, the mid-point load is 2.08 kN (Lorenzis 2009).

Table 1: Dimensions and material properties

Beam	b_1 = 1 mm	h_1 = 300 mm	E_1 = 30000 MPa
Plate	b_2 = 1 mm	h_2 = 4 mm	E_2 = 200000 MPa
Adhesive	t_a = 2 mm		

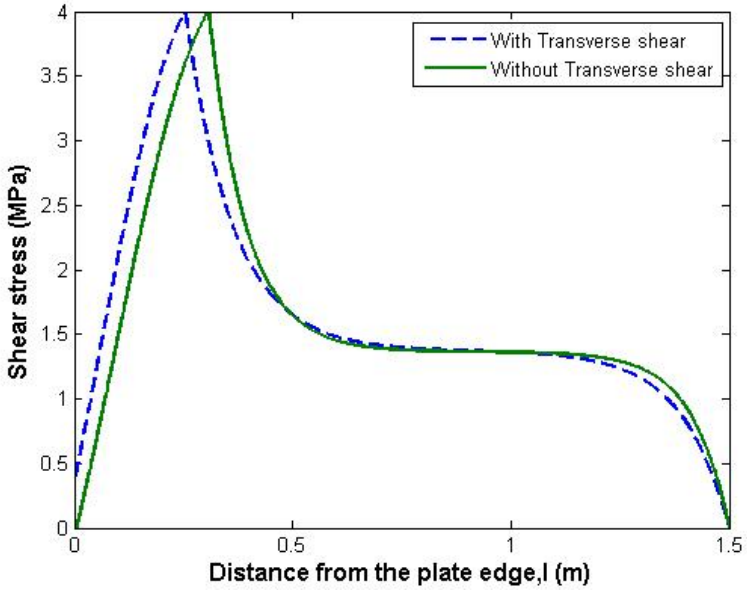

Figure 5: Interfacial shear stresses with and without transverse shear deformation

From Figure 5 it is clear that while including the transverse shear deformation of the beam and the plate, the elastic zone length increases and softening zone length decreases. Hence, it is apparent that the beam and the plate shear deformation reduces the interfacial stresses concentration and thus renders the adhesive shear distribution more uniform. The peak interfacial stresses are smaller than the stresses obtained in Lorenzis (2009). Thus the beam and the plate shear deformation is an important factor influencing the interfacial shear stress distribution.

5.1 Interfacial Shear Stress For Different Parameters

In this section, results of the present solution are presented to study the effect of various parameters namely adhesive shear strength and plate material on the distributions of the interfacial stresses in the beam bonded with FRP or steel plate. These results are intended to demonstrate the main characteristics of interfacial stress distributions in these strengthened beams. The results are presented in Figures 6–8. A summary of the geometric and material properties is given in Table 2. The plate materials considered in this study are glass fibre reinforced polymer (GFRP) composite, CFRP composite and steel.

Table 2: Dimensions and material properties

Component	Width(mm)	Depth (mm)	Young's modulus (MPa)	Poisson's ratio	Shear Modulus(MPa)
Beam	$b_1 = 200$	h_1=300	E_1=30000	0.18	
Adhesive	$b_a = 200$	t_a=2.0	E_a=3000	0.35	
GFRP plate	$b_2 = 200$	h_2=4.0	E_2=50000	0.28	$G_{12} = 5000$
CFRP plate	$b_2 = 200$	h_2=4.0	E_2=140000	0.28	$G_{12} = 5000$
Steel plate	$b_2 = 200$	h_2=4.0	E_2=200000	0.3	

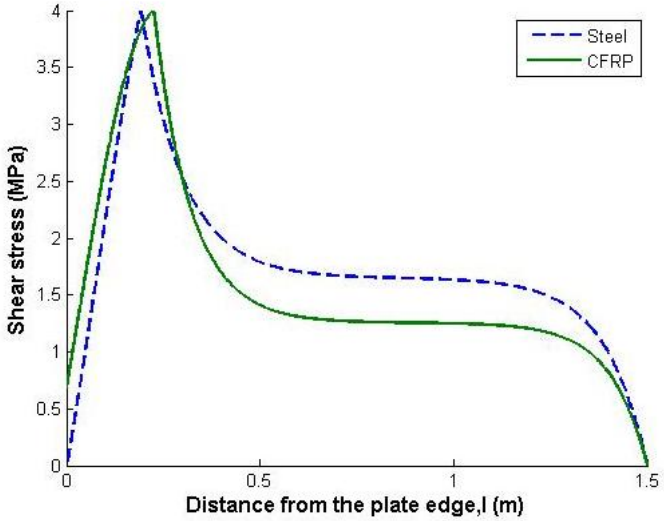

Figure 6: Effect of plate material on interfacial shear stress distribution at 2.5 kN

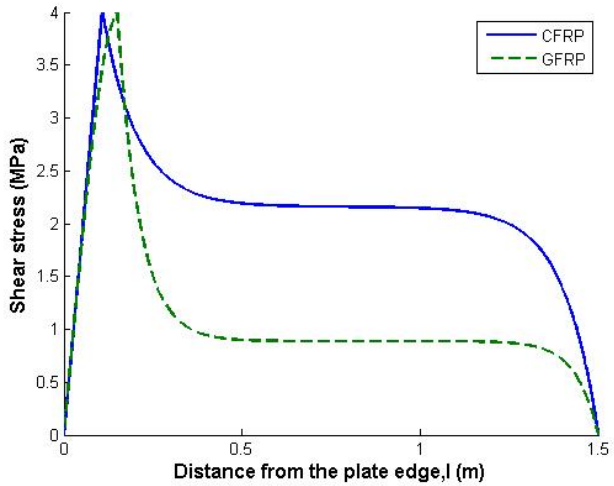

Figure 7: Effect of plate material on interfacial shear stress distribution at 4.3 kN

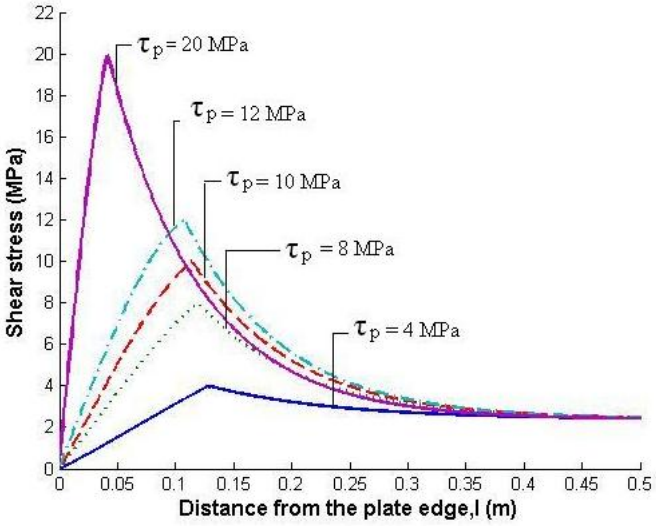

Figure 8: Interfacial stress distribution for various values of τ_p at 3.6 kN

Figures 6 & 7 represent the interfacial shear stress distribution for elastic softening and debond initiation stages. The interfacial shear stress is increased as a result of the increase in the plate elastic modulus. Figure 8 represents the interfacial shear stress behavior for various adhesives. It is clear from the plot that the elastic zone length increases and the softening region narrows as the adhesive strength value increases.

6 CONCLUSIONS

A closed form solution for interfacial stress in elastic and elastic-softening zone along with debond load is calculated using higher order theory including the transverse shear deformations of both plate and beam in a plated beam is obtained using cohesive zone integrated analytical method. The complete solution for debond initiation is presented for the case of a simply supported beam. By including the transverse shear deformation of the beam and the plate the interfacial shear stress and the softening zone decrease. Also it is observed that the softening region narrows for the adhesive with higher shear strength. The plate-end debond load increases as the plate modulus decreases.

NOMENCLATURE:

τ	Interfacial shear stress
τ_p	Peak value of shear stress
δ	Tangential relative displacement across the interface
δ_p	Tangential relative displacement at peak shear stress
δ_u	Tangential relative displacement at ultimate shear stress
K	Slope of the first portion of the cohesive law curve
G_f	Fracture energy at the interface (mode II)
P	Applied concentrated load
l	Length of the plate
a	Distance from the support to the end of the plate

b_1, b_2 Width of the beam and the plate
h_1, h_2 Depth of the beam and the plate
t_a Thickness of the adhesive
A_1, A_2 Cross-sectional area of the beam and the plate
E_1, E_2 Elastic modulus of the beam and the plate
G_1, G_2 Shear modulus of the beam and the plate
I_1, I_2 Second moment of inertia of the beam and the plate
N_1, N_2 Axial force of the beam and the plate
V_1, V_2 Shear force of the beam and the plate
M_1, M_2 Bending moment of the beam and the plate
M_T Total applied moment
V_T Total shear force
y_1 Distance from the bottom of the beam to its centroid
y_2 Distance from the top of the plate to its centroid
u_1, u_2 Tangential displacement of the beam and the plate
τ_e Interfacial shear stress in elastic stage
τ_s Interfacial shear stress in softening stage

REFERENCES

Bouchikhi A S, Lousdad A and Megueni A, "On the reduce of interfacial shear stresses in fiber reinforced polymer plate retrofitted concrete beams", Materials and Design ,Vol. 31, Issue 3, pp. 1508-1515, March 2010.

Fabrizio Greco, Paolo Lonetti, Paolo Nevone Blasi, "An analytical investigation of debonding problems in beams strengthened using composite plates", Engineering Fracture Mechanics, Vol. 74, pp. 346–372, 2007.

Laura De Lorenzis, Giorgio Zavarise, "Cohesive zone modeling of interfacial stresses in plated beams", International Journal of Solids and Structures, Vol. 46, Issue 24, pp. 4181-4191, December 2009.

Ninoslav Pesic, Kypros Pilakoutas, "Concrete beams with externally bonded flexural FRP-reinforcement: analytical investigation of debonding failure", Composites: Part B, Vol. 34, pp. 327–338, 2003.

Rabinovich O and Frostig Y, "Closed-form high order analysis of RC beams strengthened with FRP strips", American Society of Civil Engineers Journal of Composites for Construction, Vol.2, pp. 65–74, 2000.

Smith S, Teng J G, "Interfacial stresses in plated beams", Engineering Structures, Vol. 23, pp. 857–871, 2001.

Tounsi Abdelouahed, "Improved theoretical solution for interfacial stresses in concrete beams strengthened with FRP plate", International Journal of Solids and Structures, Vol. 43, pp. 4154–4174, 2006.